JPSS-1 ATMS Post-launch Active Geolocation Analysis

Cheng-Hsuan Lyu, Edward J Kim, Lisa M McCormick, Robert V Leslie, Idahosa A Osaretin

Abstract—**A NOAA-20 (N20) ATMS active geolocation test was performed around Jan. 2018 with 24 pre-selected coastline crossing scenes. After comprehensive analysis of ATMS stare data and the corresponding VIIRS data, the ATMS pitch, roll and yaw pointing angle errors are found from the nadir perpendicular, the nadir oblique shallow angle, and the off-nadir perpendicular coastline crossing data, respectively. In this study, we first determine the ATMS radiometric coastline crossing time by using the ATMS radiometric count data. Since the coastline can be located anywhere within one ATMS FOV from the passive (regular scanning) geolocation data, depending on the scan starting time, it is not a valid assumption for the inflection point being the same as the coastline location. Consequently, using the passive geolocation data to validate the sensor's on-orbit pointing angle performance is limited. After finding the ATMS radiometric coastline crossing time from the ATMS data, we compare it with the VIIRS effective time stamp (see main text). Specifically the VIIRS M3, M4 & M5 (true color) & M15 and M16 bands (thermal) data have a much smaller footprint size. Using the differences of the ATMS and VIIRS (effective) coastlines crossing times, the N20 ATMS pitch, roll and yaw pointing angle errors are found to be -0.09°, -0.24° and 0.28°, respectively. To determine ATMS geolocation properly, these on-orbit pointing errors need to be corrected, adding to the ATMS SDR Processing Coefficient Table, and passed on to the operational geolocation processing code.**

Index Terms—**Active Geolocation, Microwave radiometer, Geolocation Calibration**

I. INTRODUCTION

THE second flight unit of the Advanced Technology Microwave Sounder (ATMS), weather and climate sensor was launched aboard the Joint Polar Satellite Systems (JPSS-1 or NOAA-20, hereafter N20) satellite on Nov. 18, 2017. N20 joined S-NPP (Suomi – National Polar-orbiting Partnership) and the fleet of international polar-orbiting satellites that have been providing observations for operational weather forecasting and long-term environmental data records over the last 45 years. The ATMS is an "integrate-while-scanning" total-power-radiometer, with 96 Field Of Views (FOVs) per scan covering the frequency range of 23.8 GHz (Channel, hereafter Chan or Ch 1), 31.4 GHz (Ch 2), 50.3 – 57.3 GHz (Chs 3 – 15), 88 GHz (Ch 16), 165.5 GHz (Ch 17) and 183.3 GHz (Chs 18-22). The FOVs of the 22 ATMS channels are separated by 1.11 deg regardless of footprint sizes. The scanning geometry, swath width, and footprint dimensions are illustrated in Fig. 1. Other detailed ATMS characteristics and data product information are presented in the previous work of *Kim et al.,* [1] and *Bormann et al.,* [2]. This paper focuses on the ATMS on-orbit pointing calibration and presents the first comprehensive evaluation of ATMS pitch, roll and yaw pointing angle errors. Moreover, the ATMS and the Cross-Track Infrared Sounder (CrIS) observations are used to generate two key performance parameters (KPPs) – Atmospheric Vertical Moisture Profile (AVMP) and Atmospheric Vertical Temperature Profile (AVTP) [*JPSS ATBD CrIS Environment Data Record*, 2010]. Since the ATMS and the CrIS are currently co-aligned and co-registered (simultaneous and colocated) for JPSS-2 and to be implemented for the subsequent JPSS-3 and JPSS-4 missions, a thorough evaluation of the on-orbit pointing performance of ATMS is very important for producing accurate geolocation data.

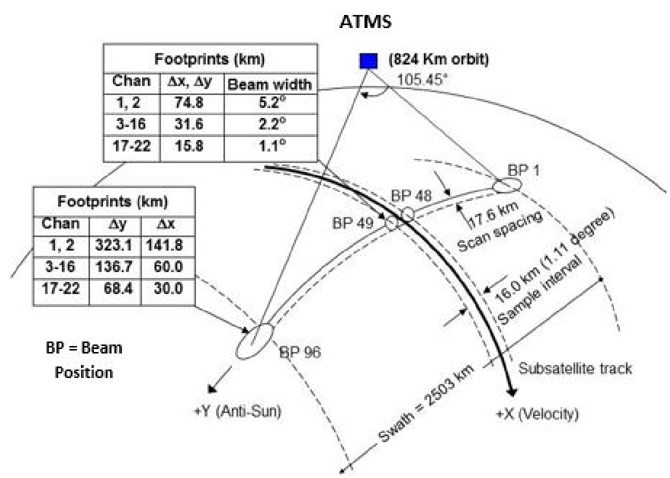

Figure 1. S-NPP & N20 ATMS Ground swath and footprint geometry.

After producing ATMS geolocation by using the operational geolocation (GEO) data processing code, there were different ways of correcting its on-orbit pointing errors. These pointing error corrections are currently missing in the GEO code. The

Cheng-Hsuan Lyu, I.M. Systems Group at NASA Goddard Space Flight Center, Code 617, Greenbelt, MD 20771, USA (e-mail: cheng-hsuan.lyu-1@nasa.gov)
Manuscript received xxx, 2019; revised xxx, 2019.

Edward Kim, NASA Goddard Space Flight Center, Greenbelt, Maryland, USA (email: Edward.j.kim@nasa.gov)
Lisa McCormick, Fibertek, Inc., NASA/GSFC, Maryland, USA
R. Vince Leslie, and Idahosa A. Osaretin, MIT Lincoln Laboratory, Lexington, Massachusetts, USA

most widely utilized geolocation validation approach uses a sensor's normal operational scan geolocated data to determine the sensor's on-orbit pointing angle errors. This is a "passive geolocation method" since no special commands are executed. It requires 1-3 months of on-orbit data collection in the case of ATMS, see Robinson [3]. Alternatively, Lambrigtsen and Lee [4] proposed a faster "active geolocation method" by using nadir stares for 24 to 48 continuous hours. The sensor's on-orbit pointing angle errors determined by using the active method are not only computed much faster and accurate but also more appropriate than those derived by the passive one. Yet, the active geolocation method involves selecting a variety of coastline crossing scenes for determining the sensor's pitch, roll and yaw pointing angle errors.

An opportunity to test the active geolocation method proposed by Lambrigtsen and Lee became available during commissioning of the N20 ATMS. The commanding had to be carefully designed. For example, if the ATMS stares too long, then the main motor will overheat (over current). For this reason, the ATMS science team selected a stare time of 1-4 minutes per segment per coastline crossing scene. This short stare was repeated for multiple crossing scenes. This strategy mitigated the potential risk of ATMS overheating due to staring and scanning at one fixed angle for longer than 24 to 48 hours. After completing this first active geolocation test on N20 ATMS, we found that an additional 2 minutes of stare for each scene might be needed for the subsequent ATMS units. This is due to uncertainty in predicting the coastline crossing time by using the Systems Tool Kit software (STK, from www.agi.com).

The paper is organized into five sections. Following the introduction in section 1, Section 2 discusses the limitations of the passive geolocation methodology applied to both S-NPP and N20 ATMS geolocation data and the potential issues for using the passive analysis. Section 3 details the use of the active geolocation method for the N20 ATMS on-orbit geolocation analysis. Section 4 presents the results of the active geolocation method for N20 ATMS. The concluding remarks in Section 5 consists of the implications of the analyses, lessons learned from data anomaly issues, and plans for using active geolocation method on subsequent ATMS flight units.

II. LIMITATIONS ON PASSIVE GEOLOCATION DATA ANALYSIS

Having some limited knowledge and unknown uncertainties in parking the on-orbit sensor to perform continuous stare for two to three days, there were no active geolocation tests on S-NPP ATMS. As a result, the instrument scientists could simply collect regularly operational scanning passive geolocation data continuously for one to three months. These passive geolocation data analysis was the only way to validate and demonstrate the on-orbit sensor's geolocation performance for S-NPP. Passive geolocation data analysis focused on the collection of appropriate coastline crossing data regions, and then a model was developed to derive the instrument's pointing angle errors.

A study on S-NPP ATMS passive geolocation method was presented by *Robinson* [3] at the NOAA S-NPP 2012 annual science team meeting. The study highlights the following five steps for passive geolocation method: (1) Pick multiple regions with high coastline contrast and orbits with coastal crossings close to nadir (Beam Positions 24 – 74); (2) Calculate the inflection point between every 4 consecutive data points in across-track rows and along-track columns; (3) Compare points to actual coast based on Global Self-consistent, Hierarchical, High-resolution Shoreline Database or GSHHS; (4) For each approximate coastline point the intersection of the perpendicular is found on the actual coast. This distance is separated into a North-South and East-West error; and (5) Accumulate error statistics for Channels 1, 3, 16 & 17.

In studying the methodology on how the on-orbit ATMS sensor scanned across the coastlines, there were some limitations on adopting the passive geolocation data to determine the sensor's pointing angle errors. Depending on the timing of when ATMS scanned across the coastline, the actual coastline position could be in any location between two ATMS FOV footprints (or ground projected FOVs), as demonstrated in Fig. 2 for the ATMS G-band (Chs 17 – 22) with 1.1º FOVs. For the G-band, at least three FOVs should be used to distinguish pure ocean and pure land view of FOV and derive the inflection point, which is assumed to correspond to the coastline location, see Fig. 2 (a) & (b). Specifically, in Fig. 2(a), A, B & C may stand for possible coastline locations from the digital map, and Fx, where x is either A, B, or C, represents the best fitted line through radiometric count inflection point. If the timing is right, the fitted Fx coastline would match the digital map coastline. In Fig. 2(b), after the maximum and minimum count data (FOVs) are determined, the middle inflection point is the coastline location. However, any one of the cases A, B and C cannot be used by itself to derive ATMS pointing angle errors. Different scan timings cause mismatch between the inflection point and the coastline. All 3 possible A, B and C and/or more different cases exist in the 2 – 3 months collected data for ATMS passive coastline crossings. Furthermore, as shown in Fig. 3, K (Ch 1), Ka (Ch 2), V (Chs 3 – 15) and W (Ch 16) bands, have larger footprints, i.e., 5.2º or 2.2º FOVs. For determining the inflection point, at least seven FOVs are required for the K/Ka bands and four FOVs are required for the V/W bands. Note also that the inflection point is defined to be the half way between a pure ocean (min. count) and a pure land (max. count) view of FOV.

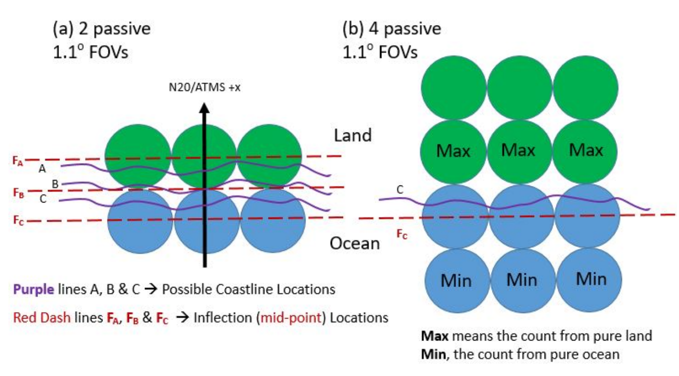

Figure 2. (a) ATMS Chs 17-22 FOVs across coastline differently at different scan starting times during its operational scan. Shown also is the corresponding inflection location. (b) Using 4 or 3 FOVs to show how we determine the inflection location.

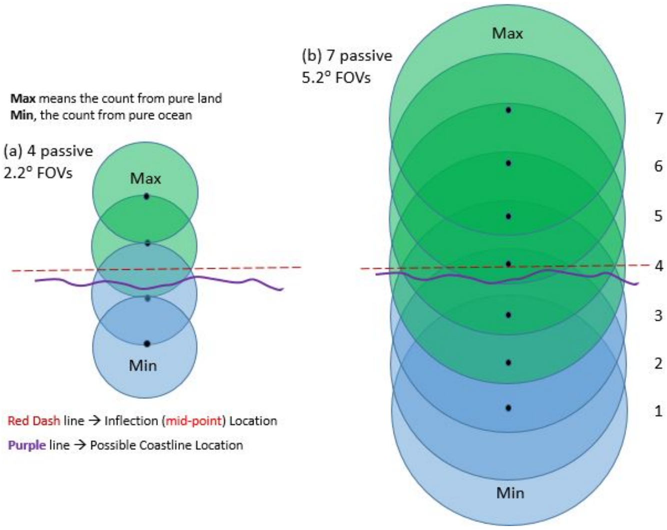

Figure 3. (a) ATMS Chs 3-16 FOVs scan across coastline location at one scan starting time. Shown also is the inflection (mid-point) location. (b) Similar case for ATMS Chs 1-2.

From the explanations above and the scan pattern demonstrations given in Figs. 2 (a) & (b) & 3 (a) & (b), the error analysis of the coastline deviation from the radiometric count inflection point reflects the statistics of the deviation (or offset) of ATMS footprints from the coastlines, because it depends on the timing when ATMS scans across the coastline regions. Since the passive geolocation data are closely associated with the scan timing, the analysis of these data would not provide actual ATMS pointing errors in terms of the pitch, roll and yaw pointing angle errors. Note that the timing for the passive scan coastline crossing also depends on the orbit control requirements that include maintenance of a repeating ground track to +/- 20 km. Most importantly, after applying all the instrument mounting and alignment coefficients in the GEO (geolocation) operational code, the geolocation validation goal is to generate more accurate geolocation data product after finding the instrument on-orbit pointing errors. Yet, for achieving this goal, the current passive geolocation data and analysis are quite limited.

III. ACTIVE GEOLOCATION TEST AND ANALYSIS

For N20 ATMS on-orbit pointing errors analysis, active geolocation tests were performed from Jan. 17 to 19, 2018 with 24 pre-selected coastline-crossing scenes after N20 reached its final orbit. These 24 scenes were equally divided into 4 different categories: (1) Nadir perpendicular coastline crossing; (2) Nadir oblique shallow angle coastline crossing; (3) +20 deg off-nadir perpendicular coastline crossing; and (4) -20 deg off-nadir perpendicular coastline crossing.

To study and calculate the sensor's on-orbit pointing angle errors, it is essential to know both the radiometric and the geometric coastline crossing times accurately. For determination of ATMS pitch and roll pointing errors, the first step is to analyze ATMS stare data from nadir perpendicular and oblique shallow angle coastline crossings separately. After finding two FOVs that show pure land and pure ocean scenes, respectively, the mid-point of these two FOVs is the radiometric coastline location and the mid-point time is the coastline crossing time. For the second step, Lambrigtsen and Lee [4] proposed to use ground processed land fraction data to determine geometric coastline crossing time. In this geometric coastline study, however, N20 VIIRS data is used to locate the coastline crossing time. VIIRS is mounted at the front section of the N20 nadir deck and ATMS is a few feet behind VIIRS. The VIIRS data, M3, M4 & M5 visible bands (combined true color image), together with M15 and M16 thermal bands have a much smaller footprint size (about 0.75 x 0.75 km, track x scan)." And this is only applicable to nadir. At the edges of scan, the footprint size becomes 1.6 x 1.6 km [5]. They are used to determine real coastline location (geometric coastline). Note that the N20 VIIRS geolocation pointing accuracy requirement is 0.375 km. The actual determined VIIRS 3σ geolocation uncertainty (accuracy) is about 0.19 km from the initial (post-launch) on-orbit calibration [6]. It is much smaller than ATMS pointing tolerance of 2 km (G band), 3.0 km (V/W bands) and 5.9 km (K/Ka bands) at nadir. Using the ATMS coastline crossing times and the information of VIIRS coastline location and its detector arrangement, we can determine the pitch and roll pointing errors. More details are described in the next paragraph. Similarly, with the stare data from off-nadir perpendicular coastline crossing, a net pointing error (vector sum) from the yaw and the pitch pointing errors are obtained. After removing the pitch pointing error, the yaw pointing error stands out. To produce accurate ATMS geolocation data, it is necessary to correct for these fixed pitch, yaw, and roll pointing errors in the ATMS SDR Processing Coefficient Table (PCT) from which the converted rotation matrix is used in the geolocation (GEO) operational code.

Moreover, before we could compare ATMS with VIIRS data, we need to determine the time series for VIIRS data. This is due to the fact that for VIIRS moderate resolution band detectors, i.e., 16 detectors, are sampled every 88.529 *μsec* simultaneously. The scan swath of these 16 detectors at nadir is about 12 *km*. After a detailed study of the VIIRS geolocated data, we find that because of the view angle (to the Earth surface) differences among these 16 detectors, we can use the difference of two scans, i.e., 1.7864 *sec*, to find effective consecutive time stamps for these detectors. It is similar to using the view angle differences to determine the corresponding geolocation. For producing the corresponding geolocation for 16 detectors, we assign the consecutive 1, 2 to 16 detectors to have an effective time stamp of 0.112, 2 x 0.112 to 16 x 0.112 *sec*, respectively. Note this time is in addition to the scan time for a given pixel, e.g., nadir position. When next scan comes, we just add 1.7864 *sec* to the time series for the same nadir scan line. This does not change the actual sampled (integration) time of slightly less than 88.529 *μsec* for each individual detector. This effective time stamp assignment corresponds to the actual view angle difference. Note also that there is no VIIRS ground scanning footprints (displacement) gap between the two consecutive scans, e.g., for the same nadir scan line. However, there could be slight gaps (underlaps) between the scans, and "serious" overlaps, depending on the satellite altitude [7]. Yet, for the near ocean level coastline areas, these gaps may not have significant impact to our analysis. As to ATMS active nadir stare scanning, since each ATMS footprint moves by 110 *m*, or 18 *msec*, as demonstrated in Figs. 4 & 5, every ATMS 200 FOVs would correspond to 2 VIIRS scans. From the VIIRS geolocation data product, we have validated that in Fig. 4(a) the assignment of the effective time stamp for all its 16 detectors is equivalent to using the view angle differences to determine the corresponding geolocation. If we, however, adopted Fig. 4(b), then it could result in as large as 5 km geolocation error to have only one time stamp or one geolocation data point for all 16 detectors. Furthermore, our analysis model would result in similar accuracy results quite comparable to the accuracy determined by other investigators [6]. They did not use one time stamp for all 16 detectors, but use all 16 individual geolocation data to convolve with the Landsat spatially degraded geolocation data. Note again that there is no time stamp involved in comparing the VIIRS geolocation with Landsat geolocation. Their determined VIIRS geolocation accuracy is about 0.19 km from their initial on-orbit calibration. Thus, it is valid to adopt Fig. 4(a) and it is quite accurate to compute the time difference between ATMS and VIIRS data for determining the deviation of the ATMS radiometric coastline crossing time from the VIIRS geometric coastline crossing time.

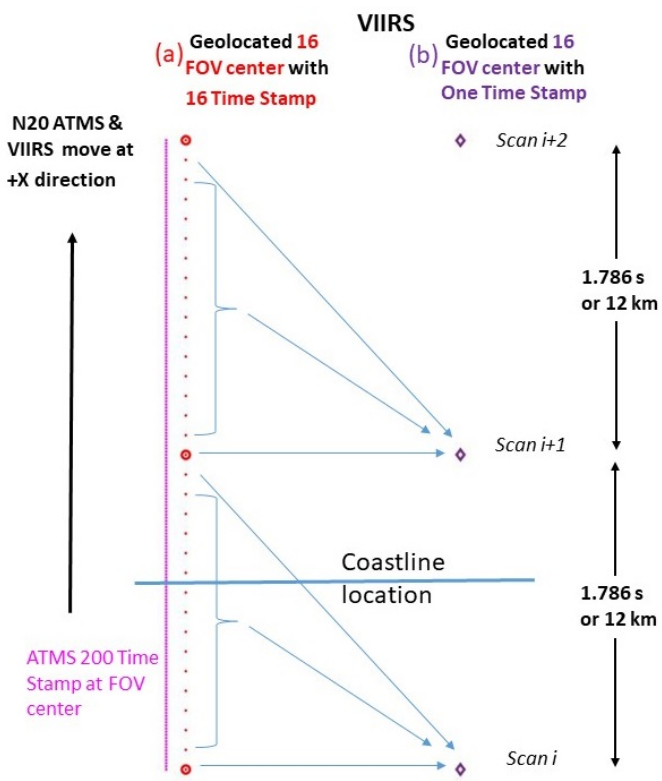

Figure 4. The overhead view of ground projected ATMS & VIIRS FOV center. (a) VIIRS 16 detectors with 16 red dots' consecutive effective time stamps & the red circle is for detector #1; the time difference of two dots is 0.112 *s*; **(b)** VIIRS 16 detectors with one raw time stamp per scan. Note cases (a) and (b) actually overlap with ATMS "nadir" scan line. For illustration purpose, we separate them. The 200 pink dots correspond to ATMS data, whose time difference of two dots is 18 *ms*; the red dots/circles and the purple diamonds correspond to VIIRS data. Fig. **4b** results in geolocation error as large as 5 km. Generating effective time stamps (Fig. 4a method) allows geolocation accuracy to within 0.375 km.

Note that the 16 effective time stamps are relative to ATMS stare time. Around the coastline crossing times, the VIIRS 16 projected ground locations/geolocations per each scan are used for this study. For some case, we may need more than one VIIRS scan. To prevent ATMS from comparing Apple (or VIIRS time) with Orange (or ATMS time), we need to determine these 16 effective time stamps, which correspond to ATMS stare time when it reached a specific VIIRS FOV, not VIIRS time stamps. Namely, it takes time for ATMS to go from VIIRS FOV#1 to FOV#16. The VIIRS 16 projected (or geolocated) FOVs are used only for distinguishing the ocean data from the land data for crossing the coastline. And the effective time stamps are not intended for use in evaluating VIIRS geolocation either.

As shown in detail in Fig. 5, in the passive geolocated scanning data, the ATMS has a scan step of 1.1 deg, equivalent to 15.8 *km* in the projected ground displacement during the operational scans near nadir for both across and along the track scanning directions. To make up for the limitations in the passive geolocation data analysis, we use the scan step of 110 *m* by the continuously diagnostic stare from the active geolocation test. This test ensures that for the analysis of ATMS pointing angle errors, the inflection location is almost identical to the actual coastline location. The error of this coastline determination is +/- 55 m, which is much better than the offset uncertainty of +/- 7.9 km from the passive geolocation data. Note this offset in the passive data is due to the sensor (relative to the coastline) start scanning time.

As illustrated in Figs. 2 and 3 for the nadir perpendicular coastline crossings, at least three crossings for the G band FOVs, four crossings for the V/W band FOVs, and seven crossings for the K/Ka band FOVs are required to determine the coastline crossing inflection locations in the passive geolocation data analysis. Here, as demonstrated in Fig. 5, for the diagnostic stare, about 3300 to 13200 FOVs (or # of data points within 1 to 4 min) were collected for each of the 21 valid coastline-crossing cases. Among all the test data points, at least approximately 300, 450 and 900 FOVs, respectively for the G, V/W and K/Ka bands, were used to determine the radiometric count inflection point or the radiometric coastline location for the same nadir perpendicular coastline crossings. As to the nadir oblique shallow angle coastline crossing scenes, e.g., for one example given in Fig. 6, at least approximately 600, 750 and 1200 FOVs, respectively, were used for similar analysis. The above-mentioned FOVs locate and distinguish the pure ocean from the pure land view data, from which we find the inflection point, i.e., the radiometric coastline location.

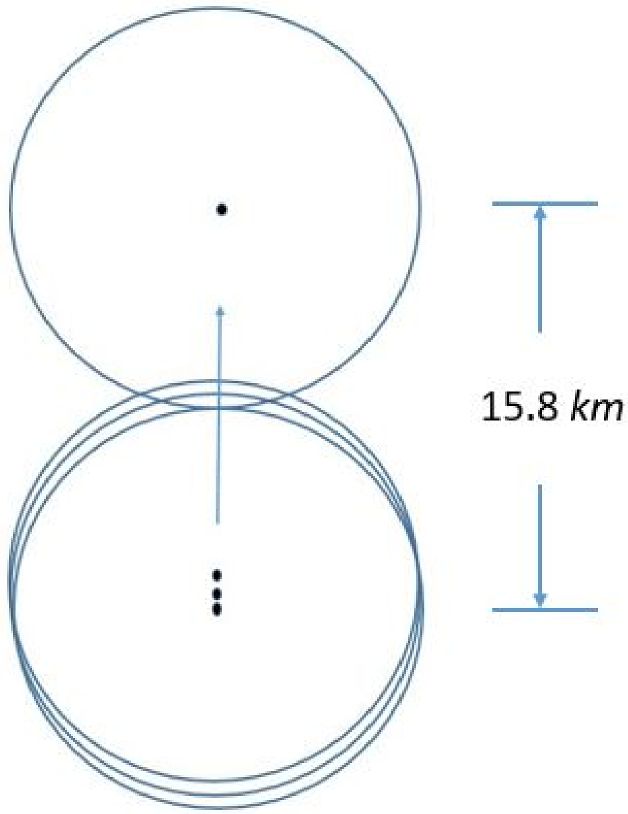

Figure 5. The ground projected FOV displacement of 110 *m* during ATMS Chs 17-22 diagnostic stare scan, compared to passive operational scan's displacement of 15.8 *km*

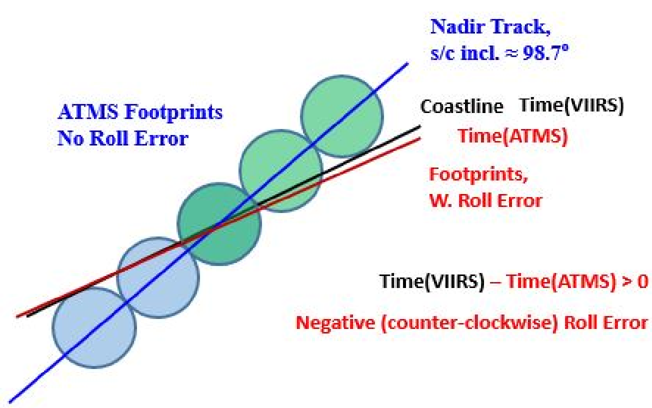

Figure 6. A case of ATMS nadir oblique shallow angle coastline crossing. Using the geometric (VIIRS) versus the radiometric (ATMS) coastline crossing times to determine ATMS roll pointing angle error.

As to the analysis of the active geolocation test data, the best ATMS channel candidates are those that see through the clouds or have less impact from the clouds and the water vapor. Based on the zenith opacity information, the relatively lowest opacity channels are Chs 1, 2, 3, 16 & 17, see Fig. 7. Thus, these five channels were chosen for ATMS radiometric coastline study. Among these five channels, Chs 1, 2, 3 and 16 are good window channels. Ch 17, 166 GHz, is sensitive to H_2O 18 *mm*, thus it is not a good window channel under all atmospheric conditions. Under the cloudless atmosphere, together with less or insignificant water vapor content in the line of sight, the measurements from ATMS Ch 17 may also result in good cases for distinguishing the pure ocean from the pure land data. See examples in Fig. 8 (a) & (b), where the pure ocean and the pure land FOVs are marked as "x", separately. The mid-point as the inflection location, i.e., the coastline location, is marked as "o". For both ATMS nadir and off-nadir stares, ATMS Chs 1, 2, 3, 16 & 17 show consistent radiometric coastline crossing times, respectively.

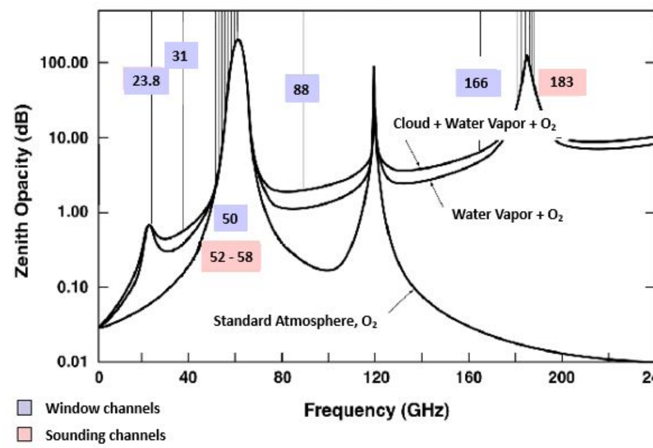

Figure 7. The zenith opacity of ATMS 22 channels. Low opacity G-band Ch 17, 166 GHz, was also selected as a potential window channel.

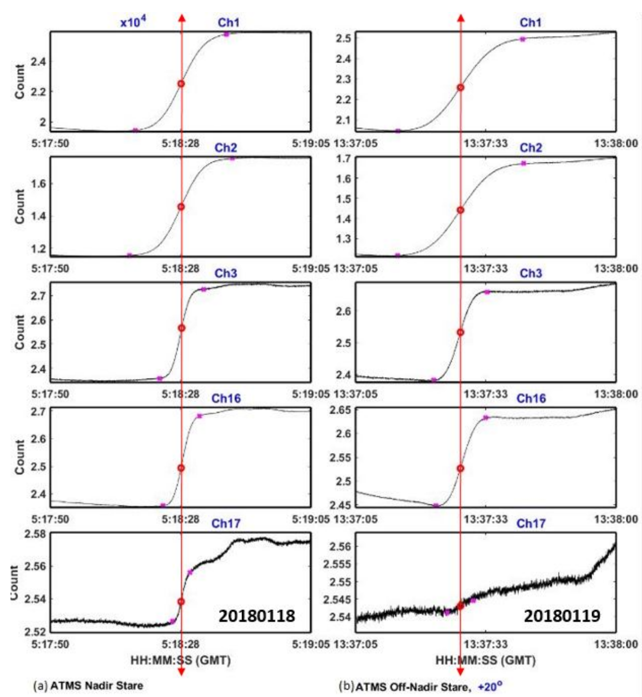

Figure 8. ATMS Chs 1, 2, 3, 16 & 17 show consistent radiometric coastline, where **o** shows the coastline location and **x** shows pure ocean & land FOVs right before & after the coastline. (a) ATMS nadir stare; (b) ATMS +20° off-nadir stare. Vertical red lines show the actual coastline location lined-up for

all 5 channels.

Another way to illustrate the significance of the results from the active geolocation test is to compare the findings with those from the simulated passive geolocation data sets. Using the data sets presented in Fig. 8, two sets of the ATMS passive (regular) scanning data are simulated and presented in Fig. 9. In the simulation, the active geolocation test stare data looks exactly like the passive scanning data after 147 data points out of every 148 data/scan were thrown out in the time series data. In either one of the two cases in Fig. 8, the first data point out of 148 data points is assumed to be the nadir or one off-nadir FOV. Note this assumption is associated with the start scan timing. In Figs. 8 (a) & (b), the simulated data show similar observations as those explained in Sec. 2. For G band, Ch 17 data, three FOV data points are needed to determine the pure ocean (min. count), the radiometric coastline location (the inflection point) and the pure land (max. count), respectively. Similarly, for determining the coastline location, eleven FOVs and five FOVs are used for the K/Ka and V/W bands, respectively. Note that the actual size of K/Ka FOV is about 5.4 deg and that of V/W FOV is about 2.4 deg. These sizes are larger than those listed in Sec. 2. The smaller FOV sizes are adopted from ATMS radiometric specifications table [8]. From Figs. 9 (a) and (b), we notice that the coastline locations determined from the simulated passive data are slightly different from those determined by the active geolocation test data. Moreover, Fig. 9 (a) seems to have a better match of the coastline location than that from Fig. 9 (b). This is simply due to the scan starting time used in the data simulation. In other words, before the simulation, if the stare starting scan were moved by a few FOVs, then the coastline location would be perfectly matched between the passive and the active geolocation data sets. From the above comparisons, it is reasonable to conclude that the passive geolocation data provides the statistics of the ATMS pointing angle deviation (offset) of finding the coastline data. Thus, the active geolocation test determines the ATMS on-orbit pointing angle errors.

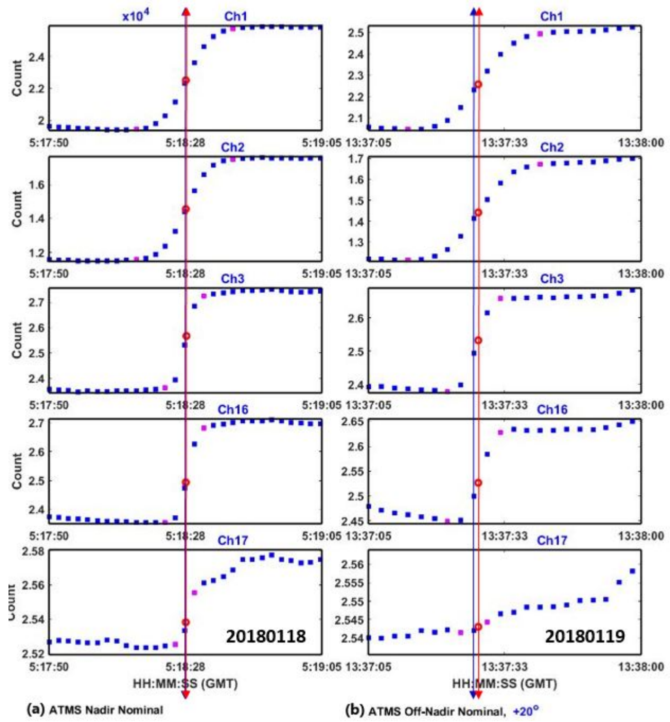

Figure 9. Blue Simulated passive regular scanning data for ATMS Chs 1, 2, 3, 16 & 17 show slightly deviated radiometric coastline, where o shows actual coastline location and x shows pure ocean & land FOVs right before & after the coastline. (a) ATMS nadir stare; (b) ATMS +20° off-nadir stare. Vertical red lines show the actual coastline location determined from the ATMS active geolocation test. Vertical blue lines show the coastline location from the simulated data.

As mentioned earlier, both VIIRS and ATMS data were used to determine the ATMS pointing angle errors, as both sensors viewed the same ground location almost simultaneously. Yet these two sensors are mounted at different locations on the N20 spacecraft nadir deck. After demonstrating how to derive the radiometric coastline crossing times with the ATMS lowest opacity window channels, the next step is to explain in detail how to derive the geometric coastline crossing times. To make sure that ATMS pointing errors are precisely derived, the VIIRS data should be able to show the coastline information accurately. As displayed in Fig. 10, both (a) VIIRS true color image as well as (b) VIIRS Long Wave (LW) thermal image show clearly the coastline crossing (the image transition points) when there is no cloud in the line of sight. To proceed with the analysis, we need to identify corresponding ATMS scanning pixels in VIIRS data.

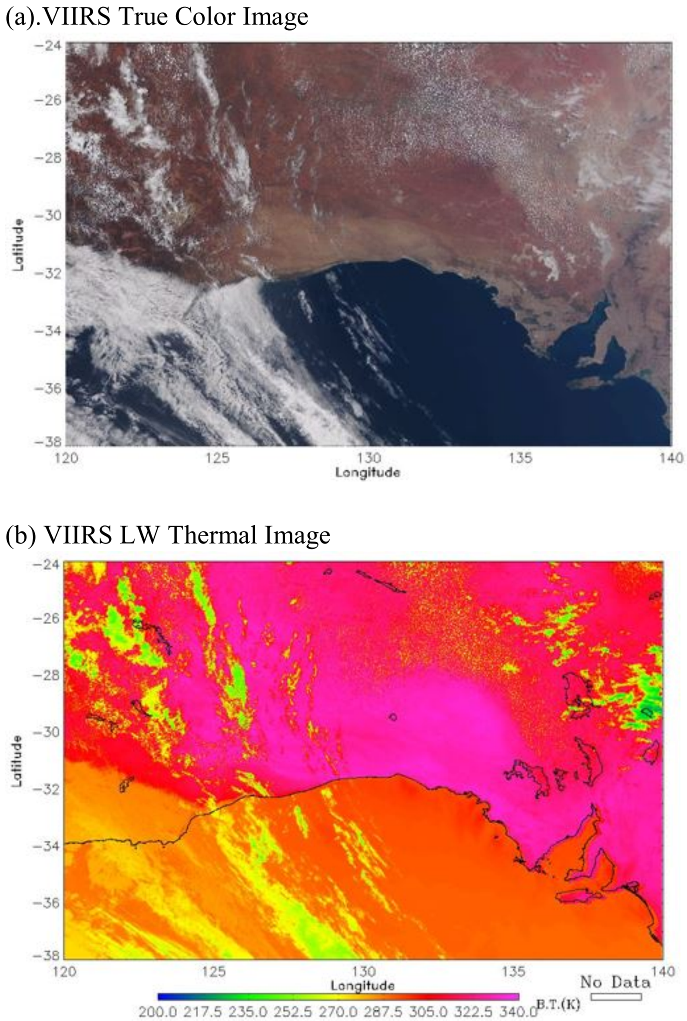

Figure 10. Either (a) VIIRS true color image or (b) LW thermal image could be used to identify the ocean and the land. Note VIIRS data were measured on 20180118_t0515_e0521.

Given one ATMS specific scan/stare of 1.1 deg. viewing angle, the corresponding VIIRS scan swath that consists of sufficient number of pixels or FOVs is shown in Figs. 11 (a) and (b). Note Figure 11(a) is not a slice image from Figure 9(b). After identifying the corresponding pixels/FOVs between VIIRS and ATMS, the next step is to compare the time series of these two different data sets. Among ATMS 24 active geolocation stare test cases, two different cases – ATMS nadir stare and ATMS +20 deg. Off-nadir stare – were selected and shown in Figs. 12 (a) and (b), respectively. For those two cases, and for the same time period of ATMS radiometric data, the geometric coastline crossing times are determined from the VIIRS thermal band data. In Fig. 12(a), showing the time sequence plot of the brightness temperature (B.T. or T_B) from the VIIRS 10763 nm data, the significant data transition is shown where the B.T. jumps by more than 25 K, from the ocean to the land. The B.T. jump time or the transition time of this VIIRS data is the geometric coastline crossing time. In Fig. 12(b), however, in the similar B.T. plot from the 10763 nm data, the B.T. jumps by only about 5 K from the ocean to the land. In this case, other features from the VIIRS data would help us to determine this 5 K B.T. jump to be the coastline crossing point.

Because emissivity is an intrinsic property of the surface, the multispectral thermal infrared emissivity data have the potential for enhancing our ability to monitor landscape changes in environmentally sensitive zones, see Hulley et al. [9]. Thus, based on Hulley (8/13/2018, private communication), the surface emissivity difference between 10763 *nm* and 12013 *nm* bands, namely the B.T. difference between VIIRS M15 & M16 thermal bands, can be used to identify the geometric coastline location. Indeed, M15 & M16 B.T. difference shows significant transition from the ocean and the land, see Fig. 12 (b) bottom plot.

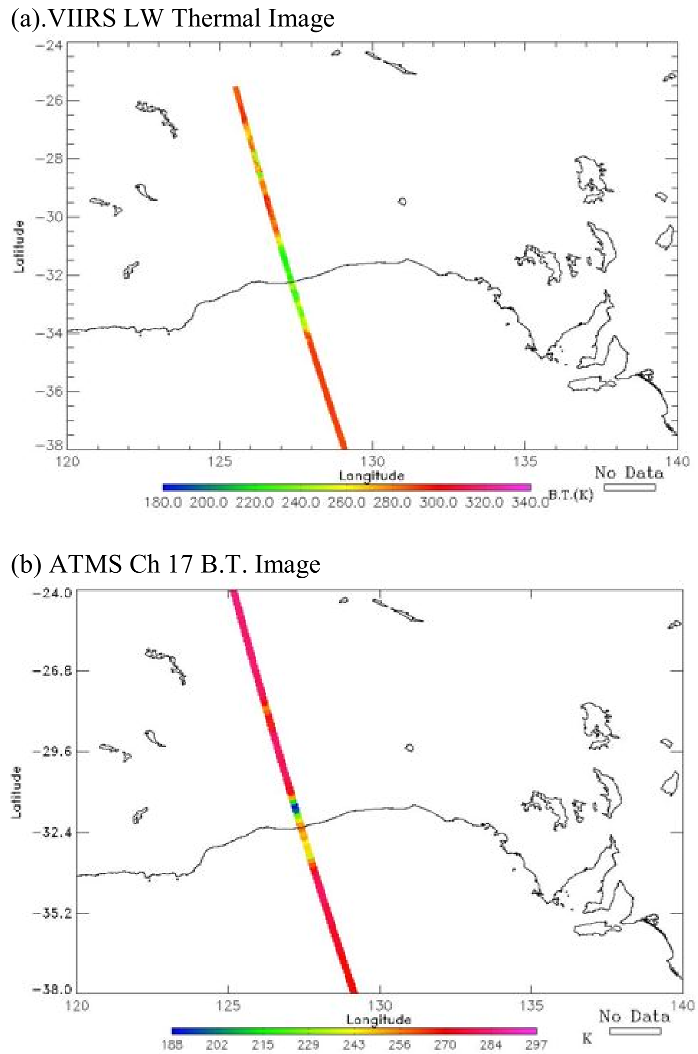

Figure 11. To compare (a) VIIRS geometric with (b) ATMS radiometric coastlines, when ATMS views the same scan swath as VIIRS. Note VIIRS data were measured on 20180203_ t0514_e0522.

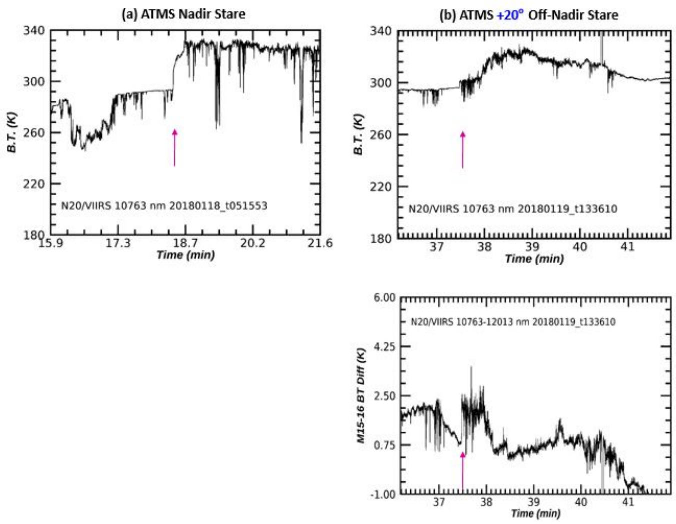

Figure 12. Active geolocation test cases (a) ATMS nadir stare; (b) ATMS +20° off-nadir stare. VIIRS geometric coastlines were identified from its thermal band data. Also for (b) the difference of M15 & M16 is another way to show the coastline data transition.

IV. OUR RESULTS

Data (21 valid out of 24 test datasets) collected from N20 ATMS active geolocation result in clear identification of the radiometric coastline crossings between the pure ocean and the pure land. Three test datasets were not usable, because the count data in these datasets showed zero counts. Since some of the pre-selected 24 scenes (datasets) have multiple coastline crossing scenarios, **5** nadir perpendicular, **7** nadir oblique shallow angle, **6** off-nadir +20° perpendicular, and **6** off-nadir -20° perpendicular coastline crossing cases are identified from all the tests. These usable cases from nadir perpendicular, off-nadir perpendicular, nadir oblique shallow angle coastline crossing show consistent results for determining ATMS geolocation pitch, roll and yaw pointing errors.

Given the fact that in areas classified as overcast, no infrared (IR) retrieval is performed. Atmospheric vertical moisture profile (AVMP) and atmospheric vertical temperature profile (AVTP) data products are derived exclusively from microwave ATMS measurements [10]. None of the twenty-two spectral bands on VIIRS, including the true color visible image and the thermal IR bands, can see through clouds. So while the VIIRS data aides in determining the geometric coastline, there are clear-view limitations. The usefulness of the VIIRS data for determining the exact geometric coastline is limited to clear sky scenes.

Consequently, from the 21 ATMS active geolocation test scenes, only 10 scenes from VIIRS are useful in determining the geometric coastline location and time. These 10 scenes contain clear sky or no visible clouds. The selections are mostly based on the fact that the VIIRS true color images, i.e., VIIRS M3, M4 and M5 bands combined images from the daytime measured data sets, are used to filter out the coastline cloud dominated data sets/scenes. For the night time collected data sets, the VIIRS thermal bands, e.g., M15 and M16, are used to filter out the cloud impacted data scenes.

The comparison of the best cases out of 10 eligible cases between ATMS and VIIRS are listed in Tables 1, 2 & 3 below:

Table 1. The Nadir Perpendicular Coastline Crossings

Coastline Crossing	Case #5 Date/Time	Case #6 Date/Time
Geometric (VIIRS)	2018-01-18/04:46:43.20	2018-01-18/05:18:28.80
Radiometric (ATMS)	2018-01-18/04:46:43.03	2018-01-18/05:18:28.54
Difference	0.17 sec	0.26 sec

Table 2. The Oblique Shallow Angle Coastline Crossings

Coastline Crossing	Case #2 Date/Time	Case #10 Date/Time
Geometric (VIIRS)	2018-01-17/19:48:00	2018-01-18/14:53:36
Radiometric (ATMS)	2018-01-17/19:47:58.51	2018-01-18/14:53:35.39
Difference	1.49 sec	0.61 sec

Table 3. The Off-Nadir Perpendicular Coastline Crossings

Coastline Crossing	Case #19 Date/Time	Case #20 Date/Time
Geometric (VIIRS)	2018-01-19/07:36:57	2018-01-19/13:37:28.80
Radiometric (ATMS)	2018-01-19/07:36:56.29	2018-01-19/13:37:28.08
Difference	0.71 sec	0.72 sec

From above Tables 1, 2 & 3, for all ATMS 5 bands, the time differences between the geometric (VIIRS) and the radiometric (ATMS) are 0.215 +/- 0.045 sec, 1.05 +/- 0.44 sec, and 0.715 +/- 0.05 sec, for the nadir perpendicular, the oblique shallow angle, and the 20° off nadir perpendicular coastline crossings, respectively. Considering the possible existence of some unknown cloudy conditions near the actual coastline areas that may have slightly affected the VIIRS geometric coastline detection, the above best (smallest) determined time differences are found to be 0.215 sec, 0.61 sec, and 0.715 sec, respectively. Note in Table 2, the measured 1.49 sec from Case # 2, may be delayed by the undetected cloud and/or water vapor content. These time differences correspond to the pitch, roll & yaw pointing errors of -0.09° (negative sign means ATMS looking down in pitch view), -0.24° (counter-clockwise roll) and 0.28° (clockwise yaw), respectively. The results are summarized in Table 4 below.

Table 4. The N20 ATMS On-orbit Pitch, Roll, and Yaw Pointing Angle Errors

Pitch (deg)	Roll (deg)	Yaw (deg)
-0.09 ± 0.02	-0.24 ± 0.10	0.28 ± 0.02

Note that the above fixed roll pointing error is in addition to the varying roll pointing deviation resulting from 96 pixel's (cross track) scan angle errors. The 96 varying scan angles are accounted for and included in the ground geolocation processing code. In short, the ATMS on-orbit determined pointing angle errors, i.e., pitch, roll, and yaw pointing errors, need to be corrected, adding to the ground measured pointing angle errors in the SDR (Sensor Data Record) Processing Coefficient Table (PCT), and passed on to the operational geolocation (GEO) data processing code.

V. CONCLUDING REMARKS

The N20 ATMS active geolocation test was an efficient way to determine the sensor's on-orbit pointing angle errors, because data collection takes 2-3 days and can be performed within 2 months of N20 satellite launch. It is most probably the fastest way that could be used to establish accurate ATMS on-orbit geolocation data product after finding and correcting the on-orbit pointing angle errors within the N20 post-launch first 90 days.

The nadir-stare mode method from the ATMS active geolocation test determines the exact time of a perpendicular coastline crossing by analyzing the closely spaced samples. The radiometric coastline crossing time is the transition time at the half-way point between the pure ocean and the pure land data. This fine stare scanning displacement on the ground is much smaller than the passive geolocation data, obtained from ATMS regular operational scanning. The centers of two neighbor-scanning footprints from the passive data are separated by 16 km, which is much larger than 110 m from the active stare data. Furthermore, for the passive geolocation data, matching ATMS FOV with the coastline depends on the scan starting time. Thus, using the passive data to validate the sensor's on-orbit pointing angle performance is quite limited.

The implemented active geolocation test required commanding ATMS into a continuous diagnostic nadir stare for 1 – 4 minutes. Utilizing the fact that several ATMS channels can see through the clouds, the instrument scientists filter the radiometer data by selecting appropriate coastline crossing scenes to determine the sensor's on-orbit pitch, roll, and yaw pointing angle errors. Using the STK tool, the active geolocation validation goal can be achieved and the nadir stare time can be reduced significantly. As shown in this study, using the STK, we have selected 24 coastline-crossing scenes and successfully adopted relatively short stare test for each coastline scene. However, when using the STK tool, the global coastline map provided by the STK was found to be rather coarse. Consequently, another additional minute or more of stare time for all the selected coastline-crossing scenes may help compensate the timing offset of the predicted coastline crossing time. Nevertheless, the currently measured data for N20 ATMS is sufficient to achieve the goal of finding the sensor's pointing angle errors. Since the assisting VIIRS sensor cannot view through clouds, we may need to select more scenes for the future sensors/missions. For the worst case scenario, when all the VIIRS data are un-usable, because of the cloudy conditions, then one alternative method is to get an ATMS FOV-averaged land fraction product (as on Aqua). Alternatively, it is also feasible to use high fidelity digital map (data is regarded as sensitive with limited access) to convolve with ATMS antenna pattern to determine the geometric coastline data/time. If one of these ancillary data is available, then the analysis is straightforward as well, see Lambrigtsen and Lee (2003 & private communication, 2018).

Based on the design of ATMS, there are two antennas or two reflectors. Yet, looking through same apertures, there are 4 feedhorns for K/Ka, V, W and G bands, respectively. From the ATMS manufacturer, Northrop Grumman, they found that there were only 3 sets, namely, K/Ka, V and W/G bands, of measured pointing angle knowledge via the ground testing. Nevertheless, there are two kinds of ATMS on-orbit geolocation data products derived from the mounting (to the spacecraft) coefficients. The science users could choose five sets of computed geolocation data products for K, Ka, V, W and G bands, respectively. Or they can choose one unique set of computed geolocation data product for all ATMS 22 channels. In this ATMS active geolocation test study, however, we find that one unique set of geolocation data product is applicable to all the chosen 5 bands of radiometric (stare) count data, see Figures 7 & 8. In other words, the coastline goes through the mid-point of the pure ocean (min) and pure land (max) for all 5 different bands. Actually, they could fit to our radiometric active geolocation model for all 24 selected coastline crossing scenes. Based on our findings, we don't even need the five (different) sets of ATMS geolocation data products. We can simply use one unique set of geolocation data product for all ATMS 22 channels.

Current and the future work for the improvement of the active geolocation test and analysis is to work closely with the JPSS MOST (Mission Operation Support Team) so that another active geolocation working plan for the subsequent sensors will be implemented properly in the future JPSS missions. This plan may include more (at least double) coastline crossing scenes of which each stare test lasts for a slightly longer time duration.

ACKNOWLEDGEMENTS

The authors wish to acknowledge the efforts of many colleagues from JPSS, S-NPP, Northrop Grumman, and NOAA over more than a decade that made the successful ATMS launch and operations possible. We would like to thank Bjorn Lambrigtsen/NASA JPL, as well as JPSS Mission Operation Support Team (MOST) for co-planning and for implementing ATMS active geolocation test. Additionally, we would like to thank the VIIRS Characterization Support Team (VCST) members: Kwofu (Vincent) Chiang, Jeffrey W. Mcintire, and Guoqing (Gary) Lin for their assistance and useful discussions about VIIRS data products and science applications. Lastly, we wish also to thank Matthew W. Sammons for his detailed review and comments.

References

[1] E. Kim, C-H. Lyu, K. Anderson, R.V. Leslie, and W. J. Blackwell, "S-NPP ATMS Instrument Prelaunch and On-orbit Performance Evaluation," *J. Geophys Res. Atmos.*, vol. 119, pp. 5653-5670, 2014.

[2] N. Bormann, A. Fouilloux, and W. Bell, "Evaluation and assimilation of ATMS data in the ECMWF system", J. Geophys. Res. Atmos., 118, 12,970–12,980, doi:10.1002/2013JD020325., 2013.

[3] K. Robinson, "Space Dynamics Laboratory (SDL) ATMS Cal/Val Tasks on Geolocation Verification and Raob Validation", Presentation on Oct. 23, 2012 at NOAA Annual Science Review, 2012.

[4] B.H. Lambrigtsen, and S.-Y. Lee, "Coalignment and Synchronization of the AIRS Instrument Suite", IEEE Trans. Geosci. Remote Sensing, vol. 41, pp. 343-351, 2003.

[5] JPSS VIIRS Geolocation Algorithm Theoretical Basis Document (ATBD), Mar. 8, 2017.

[6] S. Blonski, W. Wang, C. Cao, "Post-launch evaluation and improvements of NOAA-20 VIIRS geolocation accuracy", Proc. Of SPIE Vol. 10785, 1078518-5, 2018

[7] G Lin, R E Wolfe, J C Tilton, P Zhang, J J Dellomo, and B Tan, "JPSS-1/NOAA-20 VIIRS early on-orbit geometric performance", Proc. SPIE 10764, Earth Observing Systems XXIII, 107641H, 2018, doi: 10.1117/12.2320767.

[8] JPSS ATMS SDR Radiometric Calibration ATBD, Table 1, ATMS spectrometric and radiometric specifications, Oct. 2011.

[9] G. C. Hulley, S. Veraverbeke, S.J. Hook, "Thermal-based techniques for land cover change detection using a new dynamic MODIS multispectral emissivity product (MOD21)", Remote Sensing of Environment, 140, 755-765, 2014.

[10] JPSS Algorithm Theoretical Basis Document (ATBD) Cross-Track Infrared Sounder (CrIS) Environmental Data Record, 2010.